Title

Transient Turbulent Natural Convection in Isochoric Vertical Thermal Energy Storage Tubes: A Dimensionless Model

Journal

Journal of Thermal Science and Engineering Applications, 10(3)

ISSN

1948-5085

Authors

Lakeh, Reza Baghaei
Wirz, Richard E
Kavehpour, Pirouz
et al.

Publication Date

2018-06-01

DOI

10.1115/1.4038587

Peer reviewed

A Dimensionless Model for Transient Turbulent Natural Convection in Isochoric Vertical Thermal Energy Storage Tubes

Reza Baghaei Lakeh[1]
Mechanical Engineering Department,
California State Polytechnic University Pomona,
3801 W Temple Avenue,
Pomona, CA 91768
e-mail: rblakeh@cpp.edu

Richard E. Wirz
Mechanical and Aerospace Engineering Department,
University of California Los Angeles,
420 Westwood Plaza,
Los Angeles, CA 90095
e-mail: wirz@ucla.edu

Pirouz Kavehpour
Mechanical and Aerospace Engineering Department,
University of California Los Angeles,
420 Westwood Plaza,
Los Angeles, CA 90095
e-mail: pirouz@seas.ucla.edu

Adrienne S. Lavine
Mechanical and Aerospace Engineering Department,
University of California Los Angeles,
420 Westwood Plaza,
Los Angeles, CA 90095
e-mail: lavine@ucla.edu

In this study, turbulent natural convection heat transfer during the charge cycle of an isochoric vertically oriented thermal energy storage (TES) tube is studied computationally and analytically. The storage fluids considered in this study (supercritical CO_2 and liquid toluene) cover a wide range of Rayleigh numbers. The volume of the storage tube is constant and the thermal storage happens in an isochoric process. A computational model was utilized to study turbulent natural convection during the charge cycle. The computational results were further utilized to develop a conceptual and dimensionless model that views the thermal storage process as a hot boundary layer that rises along the tube wall and falls in the center to replace the cold fluid in the core. The dimensionless model predicts that the dimensionless mean temperature of the storage fluid and average Nusselt number of natural convection are functions of L/D ratio, Rayleigh number, and Fourier number that are combined to form a buoyancy-Fourier number. [DOI: 10.1115/1.4038587]

Introduction

Many important forms of renewable energy sources (e.g., wind and solar) are intermittent by nature. Consequently, low-cost and reliable energy storage is required to increase the dispatchability and reliability of these energy sources. Thermal energy storage (TES) is an important subsystem of concentrating solar power plants leading to greater penetration of solar power [1]. The state-of-the-art of TES for utility-scale power generation is a direct or indirect two-tank system in which a molten salt is utilized as the storage fluid. Molten salt is a suitable candidate for TES due to its low vapor pressure and high sensible heat capacity; however, increased cost of molten salt has led to elevated cost of thermal storage using conventional two-tank systems. In order to reduce the cost of TES, different materials including supercritical fluids [2–4], molten oxide glass materials [5], and elemental fluids [6–9] have been proposed as alternative storage fluids.

In this study, a dimensionless model is developed to characterize the heat transfer process in vertical thermal storage tubes. The computational results of a previous study [10] are extended and utilized to develop a dimensionless model that is able to predict the average convective heat transfer coefficient and the average temperature of the storage tube during charge cycle for different *L*/*D* configurations of the storage tube.

Computational Model, Verification, and Validation

A comprehensive description of the adopted computational model is provided in the authors' previous study [10]. An axisymmetric solution domain was utilized for the computations. Four configurations of the vertically oriented storage tubes with *L*/*D* of 4, 8, 12, and 16 are investigated. The storage fluids that are used in this study are supercritical CO_2 ($\mathrm{Pr} = 1.1$) and liquid toluene ($\mathrm{Pr} = 12.41$). The initial temperature of the storage fluids is assumed to be different in carbon dioxide and toluene computations, namely, 350 K and 250 K, respectively. A constant temperature difference of $\Delta T = 100$ K is considered between the initial temperature of the storage fluids and the outer surface of the tube wall. The governing equations of the problem are continuity, momentum, and energy. Rayleigh number values for different computations are summarized in Table 1. Previous studies on natural convection in vertical cylinders show that turbulent flow is established for $\mathrm{Ra} > 10^{11} \sim 10^{13}$ [11,12]; therefore, the buoyancy-driven flow in the storage tubes of this study is initially in the turbulent regime. The standard two-equation k–ε model is utilized to model turbulence.

A grid refinement study was utilized to verify the model and to obtain the best computational grid for the computations in Ref. [10]. The final computations were performed on a grid with 225,000 cells. In order to validate the computational model of this study, the model was adjusted and utilized to reproduce the experimental results of Evans and Reid in Ref. [12]. Figure 1 shows the computational results of the model along with experimental values extracted from Evan and Reid's paper [12]. The agreement between experimental and computational results shows that the computational model of this study is validated to predict the heat transfer characteristics in transient natural convection in vertical cylinders. Previous studies have shown that the utilized k–ε turbulence model is able to reproduce experimental data in supercritical fluids [13,14].

Results and Discussion

The configurations of flow field and temperature field are discussed in Ref. [10]. Initially, heat conducts into the storage fluid

Table 1 Rayleigh number of computations with different aspect ratio and storage fluids

L/*D*	S-CO_2	Toluene
4 ($D_i = 171$ mm)	1.77×10^{14}	2.71×10^{12}
8 ($D_i = 135.7$ mm)	7.10×10^{14}	1.03×10^{13}
12 ($D_i = 118.5$ mm)	1.60×10^{15}	2.42×10^{13}
16 ($D_i = 107.7$ mm)	2.84×10^{15}	4.31×10^{13}

[1]Corresponding author.

Contributed by the Heat Transfer Division of ASME for publication in the Journal of Thermal Science and Engineering Applications. Manuscript received October 14, 2016; final manuscript received October 19, 2017; published online January 23, 2018. Assoc. Editor: W. J. Marner.

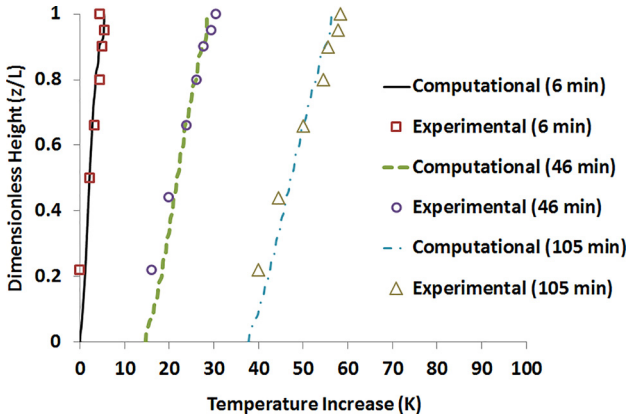

Fig. 1 Validation of the computational model with reproducing the experimental data reported in Ref. [12] for a similar configuration of parameters

from the tube wall and increases the temperature of the fluid near the wall. The buoyancy force causes the fluid to accelerate in the opposite direction from gravity and form a natural convection boundary layer attached to the tube wall. The upward flow of the heated fluid comes in contact with the top wall of the tube and is forced to move in the inward radial direction. Consequently, conservation of mass requires a downward flow at the center of the tube, forming a recirculating flow.

The attention is now turned to the buoyancy-driven heat transfer process. Figures 2(*a*) and 2(*b*) illustrate the variation of the dimensionless spatially averaged temperature of the storage fluid, θ_m, during the charge cycle as a function of Fourier number for different L/D ratios with supercritical CO_2 and toluene, respectively. The curves are terminated at the Fourier number corresponding to $\theta_m = 0.9$. The variations of dimensionless mean temperature in all four tubes show a similar trend. Steep changes of dimensionless mean temperature are shown at the start of the charge cycle which is followed by a reduction of the slope of temperature curves. Tubes with larger L/D ratio have larger Rayleigh number and exhibit steeper variation of dimensionless mean temperature versus Fourier number in both cases. The charge time criterion (i.e., $\theta_m = 0.9$) for toluene is satisfied at relatively larger Fourier numbers compared to supercritical CO_2, which is consistent with lower Rayleigh numbers associated with toluene (see Table 1).

In order to study heat transfer during the charge cycle, the variation of Nusselt number versus Fourier number for different L/D ratios and storage fluids is plotted in Figs. 3(*a*) and 3(*b*). Higher L/D ratio in both storage fluids leads to higher values of Nusselt number which is consistent with the behavior of dimensionless temperature. Changing the aspect ratio of the storage tube affects the variation of Nusselt number versus Fourier number; therefore, the L/D ratio of the storage tubes needs to be included in a comprehensive dimensionless model for the problem. The Nusselt number values of supercritical CO_2 are relatively larger than the ones of toluene, consistent with the larger values of Rayleigh number using supercritical CO_2 as the storage fluid.

Dimensionless Heat Transfer Model

In this section, a dimensionless model will be developed based on the numerical results to fully characterize the heat transfer

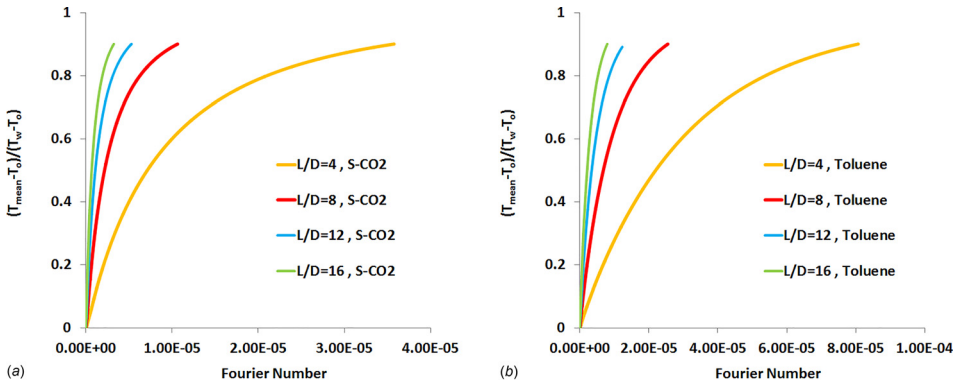

Fig. 2 (*a*) Variation of dimensionless mean temperature of the storage fluid during charge cycle for supercritical CO_2 and (*b*) variation of dimensionless mean temperature of the storage fluid during charge cycle for toluene

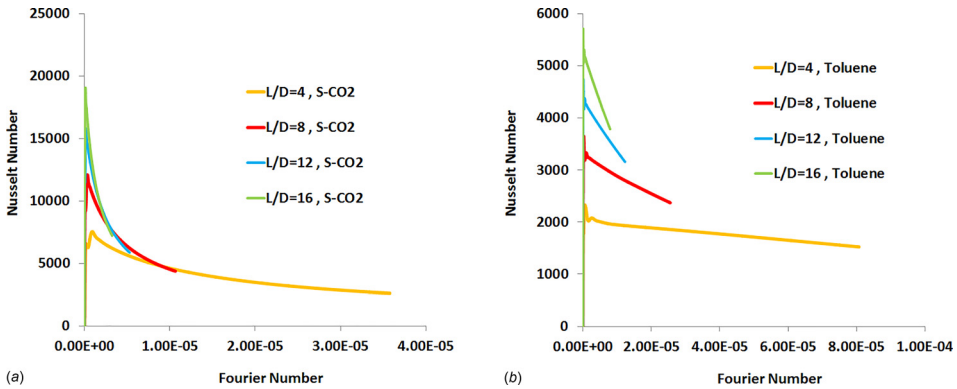

Fig. 3 (*a*) Variation of Nusselt number during charge cycle for supercritical CO_2 and (*b*) variation of Nusselt number during charge cycle for toluene

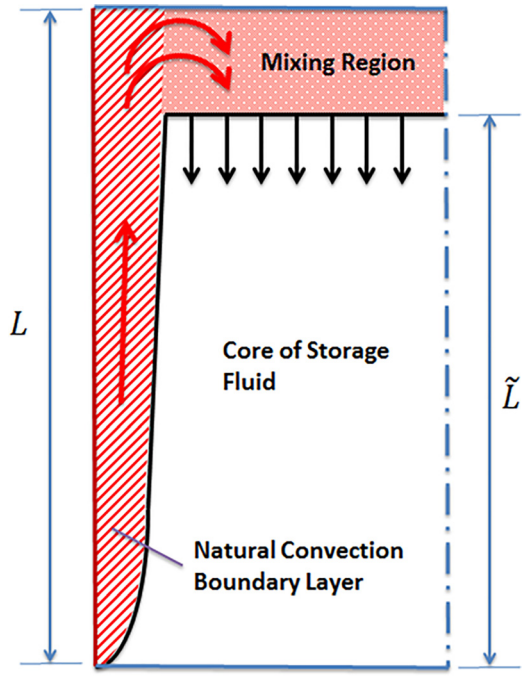

Fig. 4 Schematic of the natural convection boundary layer and different regions of the storage tube during charge cycle

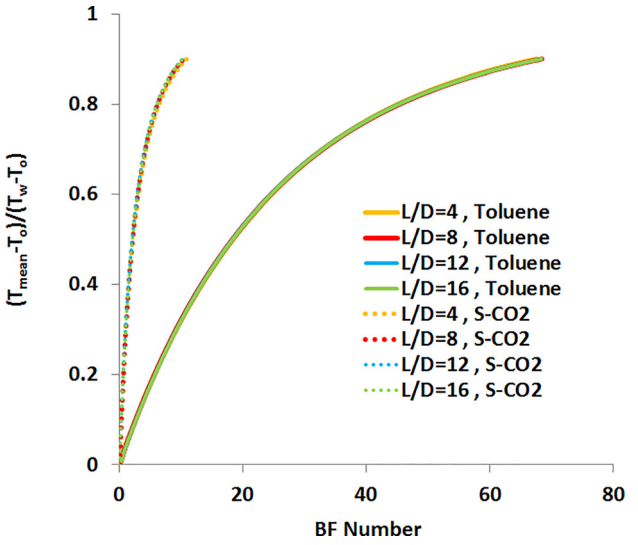

Fig. 5 Variation of dimensionless mean temperature of the storage fluid as a function of BF number for supercritical CO_2 and toluene. The results of each storage tube collapse on a single curve.

during charge cycle of an isochoric vertical thermal storage tube. The objective of this model is to find a relationship for the Nusselt number that would enable the distinct curves in Figs. 3(*a*) and 3(*b*) to collapse onto a single curve. A single curve for all *L*/*D* ratios would characterize the heat transfer due to buoyancy-driven flow during charge cycle. The model would also collapse the distinct curves of dimensionless temperature in Figs. 2(*a*) and 2(*b*) as described previously in Ref. [10].

During the charge cycle, the flow field in vertical storage tubes exhibits three regions as shown schematically in Fig. 4: (1) the thermal boundary layer attached to the tube wall, (2) the core of the storage fluid outside the boundary layer, and (3) the mixing region at the top section of the tube. The mixing region is the hottest region of the tube and in the conceptual model it is assumed to be at the constant temperature of the wall, T_w. The model also assumes that conduction from the boundary layer to the core region is negligible when compared to the rate of convection; therefore, the temperature of the core region remains at the initial temperature, T_o. The development of temperature field in all simulations shows that during charging, the accumulation of hot and buoyant flow at the top of the tube leads to propagation of the mixing region toward the bottom of the tube. At the end of charging most of the volume of the storage tube is occupied by the mixing region.

The length of the core region of the storage fluid is represented by $\tilde{L}$ which is equal to the length of the tube, L, at the start of the charge cycle and reduces with time. As the mixing region propagates toward the bottom of the tube, $\tilde{L}/L$ decreases.

The results of different studies on turbulent free convection [15,16] suggest that the Nusselt number for natural convection on a vertical surface is characterized by

$$\mathrm{Nu}_L = f(\mathrm{Pr})\mathrm{Ra}_L^m \tag{1}$$

where the function f and exponent m are determined by experimental or analytical approaches. Equation (1) will be utilized later in developing the dimensionless model to relate Nusselt number and Rayleigh number.

An energy balance suggests the following approximation for the storage fluid mean temperature, T_m during charging:

$$Mc_p \frac{dT_m}{dt} \cong \bar{h}(T_w - T_o)\pi DL \tag{2}$$

Equation (2) states that the rate of heat transfer is proportional to the temperature difference between the wall and the temperature of the core region shown in Fig. 4. It is assumed that heat transfer between mixing region and the wall is negligible because the temperature of both regions is T_w. Equation (2) was integrated and rearranged to form a dimensionless expression for the mean temperature as shown in the following equation:

$$\theta_m \cong 4\left(\frac{L}{D}\right)\mathrm{Nu}_L \cdot \mathrm{Fo}_L \tag{3}$$

Equation (1) was then utilized to relate average Nusselt number to Rayleigh number and Prandtl number. The dimensionless temperature of the storage fluid can now be expressed as shown in the following equation:

$$\theta_m \cong 4f(\mathrm{Pr}) \cdot \mathrm{BF} \tag{4}$$

where BF is the buoyancy-Fourier number defined as

$$\mathrm{BF} = \left(\frac{L}{D}\right)\mathrm{Ra}_L^m \cdot \mathrm{Fo}_L \tag{5}$$

Equations (4) and (5) suggest that the dimensionless mean temperature of the storage fluid, θ_m is a linear function of the BF number and Prandtl number; however, Eqs. (4) and (5) are derived based on the vertical flat plate assumption and not a vertical tube configuration. Therefore, it is expected that the relation between θ_m and BF does not follow the linear trend but θ_m still remains a function of BF in a nonlinear form. In Fig. 5, the dimensionless temperature θ_m is plotted as a function of BF number for all *L*/*D* ration and for both storage fluids (supercritical CO_2 and toluene). Apparently, the results of all *L*/*D* ratios collapse on a single curve for each storage fluid corresponding to different Prandtl numbers. It should be noted that supercritical CO_2 and toluene are significantly different in Prandtl number. The developed model can be utilized to find the variation of mean temperature of the storage fluid within the range of parameters tested as long as the turbulent assumption is correct.

The dimensionless model of heat transfer was further expanded by considering the definition of average Nusselt number in the equation given below:

$$\mathrm{Nu}_L = \frac{Q}{2\pi RL}\frac{L}{k\Delta T} \tag{6}$$

The convective heat transfer rate, Q, is defined by Eq. (7) based on the temperature difference between the tube wall and the core region; therefore, the heat transfer only occurs along the length of the core region, $\widetilde{L}$

$$Q = \bar{h}_{\widetilde{L}}(T_w - T_o)2\pi R\widetilde{L} \tag{7}$$

Equation (7) was then substituted into Eq. (6), and the solution is rearranged to obtain Eq. (8). The total Nusselt number Nu_L is equivalent to the partial Nusselt number, $\mathrm{Nu}_{\widetilde{L}}$, because no heat transfer is assumed to happen between tube wall and the mixing region

$$\mathrm{Nu}_L = \mathrm{Nu}_{\widetilde{L}} = \mathrm{Ra}^m_{\widetilde{L}} f(\mathrm{Pr}) = \mathrm{Ra}^m_L \left(\frac{\widetilde{L}}{L}\right)^{3m} f(\mathrm{Pr}) \tag{8}$$

Equation (8) suggests that the average Nusselt number is a function of length ratio $(\widetilde{L}/L)$ which is initially equal to 1 and decreases during charge time. The length ratio $(\widetilde{L}/L)$ is now shown to be a function of dimensionless temperature of the storage fluid. One may write the mean temperature of the storage fluid T_m in terms of the tube wall and the initial temperatures as shown in the equation given below:

$$T_m = \frac{T_w(L - \widetilde{L}) + T_o\widetilde{L}}{L} \tag{9}$$

Rearrangement of Eq. (9) shows that the length ratio $(\widetilde{L}/L)$ is a function of dimensionless temperature of the storage fluid and essentially a function of BF number as shown in the following equation:

$$\frac{\widetilde{L}}{L} = 1 - \frac{T_m - T_o}{T_w - T_o} = 1 - \theta_m = \acute{f}(\mathrm{BF}) \tag{10}$$

Since dimensionless temperature of the storage fluid θ_m is a function of BF number and Prandtl number as shown on Fig. 5, $(\widetilde{L}/L)$ is also a function of BF number. Equation (10) is now plugged into Eq. (8), and the solution is rearranged in the form of the below equation:

$$\mathrm{Nu}_L\mathrm{Ra}_L^{-m} = g(\mathrm{BF})f(\mathrm{Pr}) \tag{11}$$

Equation (11) suggests that $\mathrm{Nu}_L\mathrm{Ra}_L^{-m}$ is only a function of buoyancy-Fourier number and Prandtl number. The results of the supercritical CO_2 and toluene computations are utilized to plot $\mathrm{Nu}_L\mathrm{Ra}_L^{-m}$ as a function of BF number in Fig. 6. The curves of all L/D ratios collapse on a single curve for each storage fluid (corresponding to Prandtl Number). This behavior confirms that Nusselt number is a function of defined buoyancy-Fourier number and is inversely related to Rayleigh number. The value of exponent m is obtained by a statistical approach explained in details in Ref. [10]. The initial values of BF number for all L/D ratios correspond to the times that conduction plays a major role and the developed model (which is based on turbulent natural convection) leads to slight disagreement of the curves. Figure 6 and Eq. (11) characterize the convective heat transfer process during the charge cycle. Using the developed dimensionless method, the convective heat transfer coefficient can be approximated as long as the buoyancy-driven flow is in the turbulent regime.

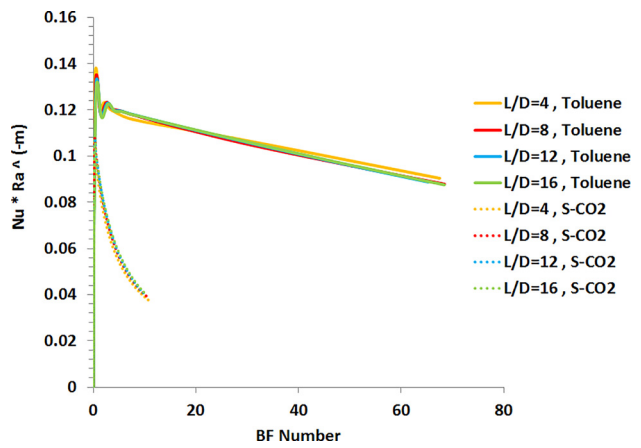

Fig. 6 Variation of Nusselt number as a function of BF number for supercritical CO_2 and toluene. The results of each storage tube collapse on a single curve.

Conclusions

In this study, the turbulent natural convection heat transfer during charge cycle of an isochoric thermal energy storage tube was studied computationally and theoretically. The thermal storage fluids (supercritical CO_2 and toluene) were chosen based on their significantly different properties and Prandtl numbers. The storage fluids were contained in sealed and vertical storage tubes. The outer surface of the storage tubes were assumed to be exposed to a constant temperature.

The results of this study show that the dimensionless mean temperature of the storage fluid and the average Nusselt number are influenced by the L/D ratio of the storage tubes in vertical orientation. Tubes with larger L/D ratio exhibit shorter charge times due to increased buoyancy-driven flow activity and larger heat transfer surface area.

A theoretical dimensionless model was developed to characterize the natural convection heat transfer process during charge cycle. The model shows that the dimensionless mean temperature of the storage fluid and the Nusselt number are functions of the BF. Assuming a turbulent buoyancy-driven flow, the developed dimensionless model can be utilized to estimate the convective heat transfer coefficient of any L/D configuration of the storage tubes.

Funding Data

- California Energy Commission (Award No. EPC-14-003).
- California State Polytechnic University, Pomona, Research, Scholarship, and Creative Activity Award (RSCA).
- Southern California Gas Company (Agreement Nos. 5660021607 and 5660042538).
- U.S. Department of Energy Advanced Research Projects Agency (DOE) (Award No. DE-AR0000140).

Nomenclature

$\mathrm{BF} = (L/D)\mathrm{Ra}_L^m \cdot \mathrm{Fo}_L$ = buoyancy-Fourier number
c_p = specific heat of storage fluid (J/kg K)
D = inner diameter of the storage tube (m)
$\mathrm{Fo}_L = (\lambda_{SF}t/\rho c_p L^2)$ = Fourier number
$g = 9.81$ = gravity (m/s^2)
$\bar{h}$ = average convective heat transfer coefficient (W/m^2 K)
L = length of the storage tube (m)
$\widetilde{L}$ = length of core region (m)
m = 0.36 = exponent
M = mass of storage fluid (kg)
$\mathrm{Nu}_L = ((q_w L)/(\lambda(T_w - T_m)))$ = average Nusselt Number
q_w = average wall heat flux to storage fluid (W/m^2)

$\mathrm{Ra} = ((g\beta L^3(T_w - T_o)\rho^2 c_p)/\mu\lambda)$ = Rayleigh number
t = time (s)
T = temperature (K)
T_m = spatially averaged temperature of storage fluid (K)
T_o = initial temperature of the storage fluid (K)
T_w = constant boundary temperature (K)

Greek Symbols

β = thermal expansion coefficient (1/K)
$\theta_m = ((T_m - T_o)/(T_w - T_o))$ = dimensionless temperature of storage fluid
λ = thermal conductivity of storage fluid (W/m K)
μ = viscosity of storage fluid (Pa·s)
ρ = density of storage fluid (kg/m^3)

References

[1] Denholm, P., and Mehos, M., 2011, "Enabling Greater Penetration of Solar Power Via the Use of CSP With Thermal Energy Storage," National Renewable Energy Laboratory (NREL), Golden, CO, Technical Report No. NREL/TP-6A20-52978.

[2] Baghaei, L. R., Lavine, A. S., Kavehpour, H. P., Ganapathi, G. B., and Wirz, R. E., 2013, "Effect of Laminar and Turbulent Buoyancy-Driven Flows on Thermal Energy Storage using Supercritical Fluids," Numer. Heat Transfer Part A, **64**(12), pp. 955–973.

[3] Baghaei, L. R., Lavine, A. S., Kavehpour, H. P., Ganapathi, G. B., and Wirz, R. E., 2013, "Effect of Natural Convection on Thermal Energy Storage Using Supercritical Fluids," ASME Paper No. ES2013-18079.

[4] Tse, L., Ganapathi, G. B., Wirz, R. E., and Lavine, A. S., 2012, "System Modeling for a Supercritical Thermal Energy Storage System," ASME Paper No. ES2012-91001.

[5] Elkin, B., Finkelstein, L., Dyer, T., and Raade, J., 2014, "Molten Oxide Glass Materials for Thermal Energy Storage," Energy Procedia, **49**, pp. 772–779.

[6] Baghaei Lakeh, R., Guerrero, Y. B., and Wirz, R. E., 2016, "Effect of Natural Convection on the Performance of an Isochoric Thermal Energy Storage System," The First Pacific Rim Thermal Engineering Conference, Waikoloa, HI, Mar. 13–16, Paper No. PRTEC-14994.

[7] Nithyanandam, K., Barde, A., Baghaei Lakeh, R., and Wirz, R. E., 2016, "Design and Analysis of Low-Cost Thermal Storage System for High Efficiency Concentrating Solar Power Plants," ASME Paper No. ES2016-59469.

[8] Nithyanandam, K., Barde, A., Tse, L., Baghaei Lakeh, R., and Wirz, R. E., 2016, "Heat Transfer Behavior of Sulfur for Thermal Storage Applications," ASME Paper No. ES2016-59470.

[9] Wirz, R. E., Stopin, A., Lavine, A. S., Kavehpour, H. P., Garcia-Garibay, M. A., Baghaei Lakeh, R., Tse, L. A., Furst, B., and Bran-Anleu, G., 2015, "High-Density, High-Temperature Thermal Energy Storage and Retrieval," The Regents of The University of California, Oakland, CA, U.S. patent No. US20150060008 A1.

[10] Baghaei Lakeh, R., Lavine, A. S., Kavehpour, H. P., and Wirz, R. E., 2015, "Study of Turbulent Natural Convection in Vertical Storage Tubes for Supercritical Thermal Energy Storage," Numer. Heat Transfer, Part A, **67**(2), pp. 119–139.

[11] Papanicolaou, E., and Belessiotis, V., 2002, "Transient Natural Convection in a Cylindrical Enclosure at High Rayleigh Numbers," Int. J. Heat Mass Transfer, **45**(7), pp. 1425–1444.

[12] Evans, L. B., and Reid, R. C., 1968, "Transient Natural Convection in a Vertical Cylinder," AIChE J., **14**, pp. 251–259.

[13] Sharabi, M. B., Ambrosini, W., and He, S., 2008, "Prediction of Unstable Behaviour in a Heated Channel With Water at Supercritical Pressure by CFD Models," Ann. Nucl. Energy, **35**(5), pp. 767–782.

[14] Roelofs, F., 2004, "CFD Analyses of Heat Transfer to Supercritical Water Flowing Vertically Upward in a Tube," Netherlands Ministry of Economic Affairs, Netherlands Ministry of Economic Affairs, The Hauge, The Netherlands, Technical Report No. NRG 21353/04.60811/P.

[15] Bayley, F. J., 1955, "An Analysis of Turbulent Free-Convection Heat-Transfer," Proc. Inst. Mech. Eng., **169**, pp. 361–370.

[16] Vliet, G. C., and Ross, D. C., 1975, "Turbulent Natural Convection on Upward and Downward Facing Inclined Constant Heat Flux Surfaces," ASME J. Heat Transfer, **97**(4), pp. 549–554.